Macromolecules

Article

pubs.acs.org/Macromolecules

Analytical and Simulation-Based Models for Drug Release and Gel-Degradation in a Tetra-PEG Hydrogel Drug-Delivery System

Ralph Reid,[†] Miriam Sgobba,[‡,§] Barak Raveh,[‡] Giulio Rastelli,[§] Andrej Sali,[‡] and Daniel V. Santi*[,†]

[†]ProLynx, San Francisco, California 94158, United States

[‡]Department of Bioengineering and Therapeutic Sciences, Department of Pharmaceutical Chemistry, and California Institute for Quantitative Biosciences (QB3), University of California, San Francisco, San Francisco, California 94143, United States

[§]Dipartimento di Scienze della Vita, Università di Modena e Reggio, 41121 Emilia, Italy

Supporting Information

ABSTRACT: We have recently reported drug-releasing, degradable Tetra-PEG hydrogels as a new drug delivery system. The gels contain two self-cleaving β-eliminative linkers: one that covalently tethers the drug to the gel and releases it at a predictable rate, and another with slower cleavage that is installed in each cross-link of the polymer to control gel degradation. By balancing the two cleavage rates, the system can be designed to discharge most or all of the drug before the gel undergoes significant degradation. If polymer degradation is too rapid, undesirable gel-fragments covalently bound to the drug are released; if too slow, the gel remains in the body as an inert substance for prolonged periods. Here, we describe an analytical theory as well as a Monte Carlo simulation of concurrent drug release from and degradation of Tetra-PEG polymers. Considerations are made for an ideal network as well as networks containing missing bonds and double link defects. The analytical and simulation approaches are in perfect agreement with each other and with experimental data in the regime of interest. Using these models, we are able to (a) compute the time courses of drug release and gel degradation as well as the amount of fragment−drug conjugate present at any time and (b) estimate the rate constants of drug release and gel degradation necessary to control each of the above. We can also account for the size-dependent elimination of gel fragments from a localized semipermeable compartment and hence estimate fragment mass vs time curves in such in vivo compartments. The models described allow design of an optimal Tetra-PEG drug delivery vehicle for a particular use.

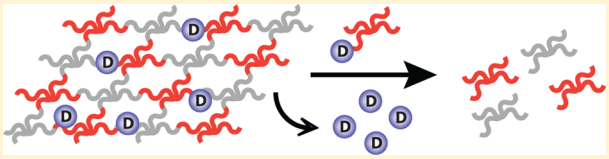

INTRODUCTION

A highly homogeneous hydrogel network—termed a "Tetra-PEG" hydrogel—with extraordinary mechanical strength has recently been developed.[1] The polymer is made by polymerizing stoichiometric amounts of two types of four-arm poly(ethylene glycol) (PEG) molecules having different end groups, A and B; end group A only reacts with B, and B only with A, to form a near-ideal network that resembles the diamond lattice with few cross-linking defects or entanglements (Figure 1A).

We have recently developed a drug-delivery system in which a drug is covalently tethered to a Tetra-PEG hydrogel network via linkers that self-cleave at predictable rates by β-elimination reactions.[2] Similar β-eliminative linkers are also used to cross-link the polymer to give gels that degrade at predictable rates (Figure 1). By using one β-eliminative linker to tether a drug to the hydrogel, L1, and another with a slower cleavage rate to control polymer degradation, L2, the system can be coordinated to release the drug before the gel undergoes significant degradation. As these gels degrade, single Tetra-PEG units, or "monomers"—which require cleavage of only four L2 bonds—are the first fragments formed (Figure 1B); as additional bonds are cleaved over time, larger fragments requiring cleavage of more than four bonds appear, each made up of covalently attached tetra-PEG units; we refer to these fragments as "oligomers". Fragments are formed with or without attached drug and depending on size may diffuse from the bulk gel. Ultimately, all fragments and fragment−drug conjugates are converted to free drug and monomers.

In this drug delivery system, the first-order rate constants of drug release, k_1, and hydrogel degradation, k_2, need to be optimally balanced so that the drug is largely released before the gel undergoes significant degradation. Otherwise, excessive fragments of gel will be solubilized that are covalently bound to the drug; although the drug will ultimately be released from such transient fragments they may have undesirable properties and should be minimized. Nonetheless, polymer degradation should be as fast as practical, so the gel does not remain in the *in vivo* compartment as an inert substance for unnecessary periods. This goal requires coordination and balancing of the rates of hydrogel degradation and drug release, and an assessment of the amount of free drug released versus the amount that is still fragment-bound. Thus, quantitative models of the macroscopic behaviors of Tetra-PEG polymers and their drug-conjugates during the degradation process are needed. A number of models of gel degradation[3−5] and drug-release from

Received: July 20, 2015
Revised: September 4, 2015
Published: September 30, 2015

DOI: 10.1021/acs.macromol.5b01598
Macromolecules 2015, 48, 7359−7369

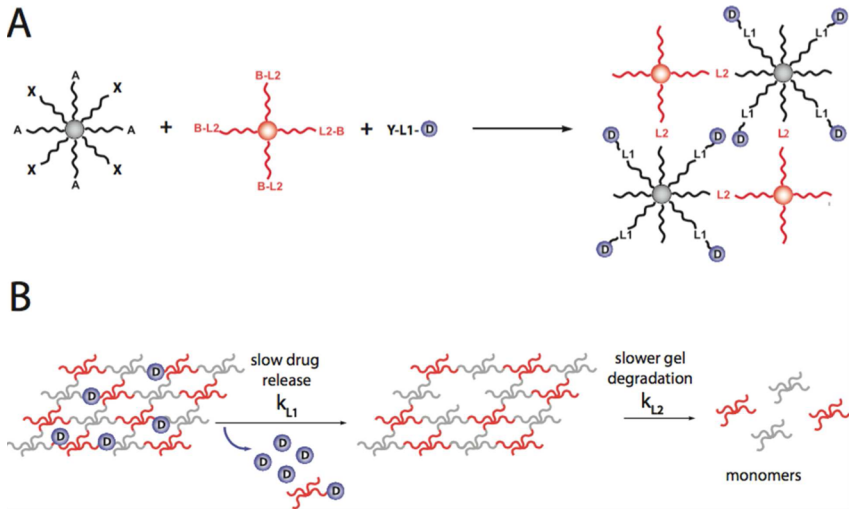

Figure 1. (A) Synthesis and structure of drug-releasing Tetra-PEG hydrogels. A and B are connecting end-groups on monomers for polymer formation, X and Y are connecting groups for attaching a drug linker to the gel, and L1 and L2 are β-eliminative linkers connecting the drug D to the gel and forming the cleavable cross-links of the gel, respectively. (B) Depiction of drug release and degradation of a Tetra-PEG gel.

polymers tethered to drugs[6,7] have been reported. However, in general, such approaches are not sufficient for our present purposes and do not provide methods to estimate subpopulations of degradation fragments.

The present work develops models—both an analytical theory and a Monte Carlo simulation—for the concurrent release of covalently bound drugs from the polymers and degradation of Tetra-PEG polymers as well as for estimation of transient fragment−drug conjugates formed over the period of gel degradation. Using these, we are able to compute the amounts of the free drug released from the gel and its fragments as well as the levels of soluble drug-fragment conjugates. From these, we can estimate the balance of k_1 and k_2 necessary to achieve the desired amount of free drug released from the gel and restrict the fragment−drug conjugates present at any time, thus enabling design a hydrogel-drug conjugate with desired properties. With adjustments for presumed gel-imperfections—unformed bonds or primary double links—the models show excellent fits to available experimental data. Finally, we describe models in which polymer fragments of specified sizes formed in vivo during gel degradation escape semipermeable compartments, and use these to describe anticipated fragment mass vs time curves in such compartments.

RESULTS

Much of the work on gel degradation is on gels not of the Tetra-PEG type and is either not directly applicable to our gels of interest or fails to exploit the special properties of this type of gel. The extensive work of Sakai and collaborators on Tetra-PEG gels[1a,b] includes methods to predictably control the time of reverse gelation,[4] but does not model the mass degradation time course. None of the previous models provide methods to estimate subpopulations of degradation fragments relevant to analyzing drug delivery in semipermeable compartments. Below is a description of the rationale and approaches used to compute Tetra-PEG gel degradation and drug release; complete derivations of equations and methods are presented in Supporting Information.

In the approach used here, we assume that (1) the ideal Tetra-PEG gel structure resembles the diamond lattice, (2) fractions of A and B end groups near the gel surface ("edge") are negligible compared to the total A−B groups within the network, (3) gel defects are primarily due to initially unformed bonds and primary "double links", (4) rate constants k_1 and k_2 are uniform in the intact gel and fragments formed, and (5) fragments formed by gel degradation up to at least hexamers can freely diffuse from the degrading gels. The latter assumption was experimentally verified by showing that at 37 °C PEG oligomers up to 8-fold the molecular weight of a Tetra-PEG monomer diffuse from the encapsulating Tetra-PEG gel with a $t_{1/2}$ of ≤35 min; the gels of interest here degrade over much longer periods, so diffusion of such oligomers from the gel is not kinetically relevant.

I. Analytical Models. *1. Analytical Model of Hydrogel Degradation. A. Fragment Formation during Degradation.* To estimate the probability that an oligomer of size N is released from the gel, it is necessary to know the number M of bonds that need to be broken and the number B that need to be kept intact. For any size oligomer N, there are a small number of subtypes that we designate as L, N, and D, with each having a fixed M and B. If the rate constant for cross-link L_2 cleavage is k_2, any L_2 bond initially present has a probability $p_{L2,t} = e^{-k2t}$ of being intact at time t. The probability $P_t(N,L,D)$ that a randomly chosen monomer is in a fragment of type N, L, and D is

$$P_t(N, L, D) = Q_{NLD} p_t^{\,B} q_t^{\,M} \quad (1)$$

Integer L is the number of independent closed loops within an oligomer, corresponding to the number of bonds that can be cleaved without fragmenting the oligomer; it depends on the topology of the graph associated with the oligomer. $B = N + L - 1$ is the number of unbroken bonds in the oligomer. Integer D is the number of bonds already broken between monomers in the oligomer; it depends on the topology of the graph as a subgraph of the diamond lattice. $M = 2N + 2 - (2L + D)$ is the number of broken bonds. Q is the number of oligomers of size N that contain a given monomer and are characterized by L and D. Supporting Table S1 provides B, M, and Q values, as well as (N,L,D) types found in fragments with $N \leq 12$.

The variable p_t is the probability that a cross-link bond is present at time t during degradation; here, f is the fraction of

DOI: 10.1021/acs.macromol.5b01598
Macromolecules 2015, 48, 7359−7369

bonds not intact at the time of initiation, which for an ideal hydrogel is zero:

$$p_t = (1 - f) \times e^{-k_2 t} = (1 - f) \times p_{L2,t} \quad (2)$$

q_t is the probability that a bond is absent at time t:

$$q_t = 1 - p_t \quad (3)$$

Thus, eq 1 can be expanded to

$$P_t(N, L, D) = Q_{NLD} p_t^{N-1+L} q_t^{2N+2-(2L+D))} \quad (4)$$

The probability, $P_{N,t}$, that a monomer is free or contained in a free oligomer of size N can be calculated at any time throughout gel degradation by summation of the probabilities of subtypes of size N:

$$P_{N,t} = \sum_{L,D} Q_{NLD} p_t^{N-1+L} q_t^{2N+2-(2L+D)} \quad (5)$$

Table S2 lists $P_{N,t}$ expressions for oligomer sizes $N \leq 6$. For the remaining sizes of $N \leq 12$, the expressions $P_{N,t}$ are straightforward to construct from the values of B, M, and Q given in Table S1 by substitution into eq 5. $P_{N,t}$ gives the fraction of mass present in the oligomers of size N at any time; thus, the sum, $\Sigma P_{N1-6,t}$, gives the cumulative fraction of total gel mass in oligomers of size 1−6.

The time of reverse gelation t_{RG}, is the time at which the initially intact bonds are reduced below a certain critical fraction (p_c) and the gel becomes completely soluble; it is an important descriptor of degradable gel polymers. The t_{RG} for many gels approximates the half-life of the cleavable bonds of the polymer.[3] Tetra-PEG gels are unusually uniform in structure and have been suggested to approximate the structure of the diamond lattice, for which the critical fraction (p_c) is ∼0.39.[8] Thus, a perfect Tetra-PEG gel does not dissolve until ∼61% of the bonds are broken; t_{RG} is therefore somewhat larger than $t_{1/2}$ of the cleavable cross-links.

Figure 2A shows estimated total gel degradation vs time, compared with calculated curves of mass in free monomers ($P_{1,t}$), selected oligomers ($P_{N.t}$), fragments of size 1−6 ($\Sigma P_{N1-6,t}$), and fragments of size 1−12 ($\Sigma P_{N1-12,t}$). The time on the x-axis is normalized by the time of reverse gelation (t/t_{RG}). The monomers and examples of individual oligomers present throughout degradation show the degree to which smaller fragments form before larger ones. After t_{RG}, maxima characteristic of each oligomer size N occur, earlier for larger than smaller oligomers. Subsequently, cleavage to smaller oligomers predominates and all mass is eventually converted to monomers. Sums of oligomers $N \leq 6$ and $N \leq 12$ form in similar amounts until ∼$0.7t_{RG}$ when they begin to diverge (at $0.5t_{RG}$, the sum for $12 \geq N > 6$ is nearly 100-fold less than the sum for $N \leq 6$, and less than 0.04% of total mass; by $0.7t_{RG}$, this ratio of 100 decreases to ∼12 and the amount increases to ∼0.9% total mass). At each time point, the amount of each larger fragment size $N > 12$ formed is predicted to decrease rapidly with size,[9] few are expected to materialize during this period. Hence, until ∼$0.7t_{RG}$ oligomers $N \leq 6$ provide a good estimate of total degraded products formed and diffused away. As degradation proceeds from $0.7t_{RG}$ to t_{RG}, significant amounts of larger fragments begin to form. Thus, the curve from $0.7t_{RG}$ to $1.0t_{RG}$ should rise with increasing steepness, eventually approaching the vertical as it nears t_{RG}. The pore size increases as degradation proceeds, allowing increasingly larger fragments to escape the gel.

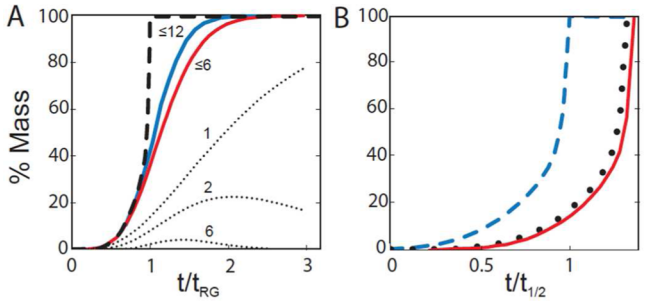

Figure 2. Gel degradation computed by analytical theory. (A) Mass loss of an ideal gel (---), with calculated time courses (using eq 5) of fractions of mass in small fragments for $N \leq 6$ (red −), $N \leq 12$ (blue −), and selected fragment sizes N = 1, 2, and 6 as labeled. The early portions of the curve for total mass loss are calculated from our methods; the remaining near-vertical portion is sketched by hand. (B) Mass loss of ideal gel (red −), gel with 22% missing bonds (blue ---), and gel in which 25% monomers have double links (• • •). The dashed and dotted lines are sketched by shifting the solid line to the left to match the calculated $t_{RG}/t_{1/2}$ predictions (ideal gel, $t_{RG}/t_{1/2}$ = 1.36; 25% double links, 1.32; 22% missing bonds, 1.00).

B. Effect of Gel Defects on Degradation. Tetra-PEG gels usually possess defects that can modify their properties, the most common being unformed bonds and primary double links.[10] Considered below are effects of these defects on the time-course of degradation and t_{RG}.

a. Unformed Bonds. For these defects, gels are modeled on the diamond lattice with the exception that they exhibit a randomly distributed initial fraction, f, of unformed bonds. Degradation of such a gel is equivalent to the degradation of an ideal gel once it has been allowed to degrade to the point where f bonds are broken. Thus, the net effect is that the degradation curve of the ideal gel in Figure 2B is shifted to the left and the apparent t_{RG} is reduced. The initial fraction of intact bonds is $(1 - f)$; the fraction of intact bonds, p_t, at time t is $(1 - f)(e^{-k_2 t})$ (eq 2). Applying these values in eq 1 gives the degradation curves for fragments of all NLD types.

The degelation point is reached when the fraction of intact bonds p_t is reduced to the critical fraction 0.39 as in eq 6:

$$p_t = 0.39 = e^{-k_2 t_{RG}}(1 - f) \quad (6)$$

If p_c is defined as the fraction of initially intact bonds still intact at degelation, then

$$p_c = e^{-k_2 t_{RG}} \quad (7)$$

Combining eqs 6 and 7 gives $p_c = 0.39/(1\text{-}f)$ for the gel with f initially unformed bonds. Substituting $p_c = 0.39/(1 - f)$ in eq 7, and replacing k_2 by $\ln 2/t_{1/2,L2}$, gives

$$t_{RG} = t_{1/2,L2} * \frac{\ln\left[\frac{(1-f)}{0.39}\right]}{\ln 2} \quad (8)$$

Thus, when $f = 0$, the hydrogel is ideal with p_c = 0.39 and t_{RG} = $1.36t_{1/2,L2}$. For gels with 22% unformed bonds, p_c is ∼0.5 and $t_{RG} \sim 1.00t_{1/2,L2}$.

b. Primary Double Links. In a second-level approximation, we allow two connecting bonds between adjacent monomers - termed primary double links. Considered below are effects of double-links on t_{RG} and the time-course of degradation.

DOI: 10.1021/acs.macromol.5b01598
Macromolecules 2015, 48, 7359−7369

Calculations on the effects of unformed bonds on t_{RG} (eq 8) can be adapted to allow the possibility of double links with or without unformed bonds. Assume a fraction f_2 of bonds of the ideal structure are converted to double links, with a second fraction f_3 remaining as single bonds. Because no monomer may have more than four bonds, graph theory requires $f_3 + 2f_2 \leq 1$ and leaves $2(1 - f_3 - 2f_2)$ free arms. In analogy to the case with unformed bonds with no double links, where each unformed bond corresponds to two free arms, we define f_1 = (free arms)/2, which implies $f_3 = 1 - f_1 - 2f_2$.

Reverse gelation of a diamond-lattice gel with random missing bonds occurs when the probability that a pair of adjacent nodes has at least one link between them is 0.39. For the fraction f_3 initially linked by a single bond, this probability is p_c. For the fraction f_2 initially linked by two bonds, the probability is $1 - (1 - p_c)$.[2] Setting the sum of $f_3 p_c$ and $f_2(1 - (1 - p_c)^2)$ equal to 0.39 implies that p_c must satisfy eq 9, which is quadratic when $f_2 > 0$. If $f_2 = 0$, the equation gives $p_c = 0.39/(1 - f_1)$, as for the case of unformed bonds:

$$f_2 \times (p_c)^2 - (1 - f_1) \times p_c + 0.39 = 0 \tag{9}$$

When $f_2 > 0$, solving the equation for p_c gives

$$p_c = \left(\left(\frac{f_3}{2f_2}\right) + 1\right) - \sqrt{\left(\left(\frac{f_3}{2f_2}\right) + 1\right)^2 - \left(\frac{0.39}{f_2}\right)} \tag{10}$$

where $f_3 = 1 - f_1 - 2f_2$. Substituting p_c from eq 10 into eq 7 gives

$$t_{RG} = \frac{-\ln\left[\left(\left(\frac{f_3}{2 * f_2}\right) + 1\right) - \sqrt{\left(\left(\frac{f_3}{2 * f_2}\right) + 1\right)^2 - \left(\frac{0.39}{f_2}\right)}\right]}{\ln 2} \times t_{1/2,L2} \tag{11}$$

thus providing t_{RG} for a hydrogel with mixed unformed and double links.

The effect of double links on t_{RG} is expected to be small in experimental gels. If 25% of monomer units are in double links—but without other defects such as triple bonds or free unattached arms—application of eq 11 predicts $t_{RG} \sim 1.32 t_{1/2,L2}$; Figure 2B compares the small effect on t_{RG} of this 25% level of double links to the much larger effect predicted for 22% missing bonds. The minimal effect of double links is expected from the balance between two effects: creation of a double link requires absence of a single link, thus decreasing the number of linked pairs to be separated before reverse gelation; in addition, a pair of monomer units that are double-linked is slower to separate. The fraction of monomers in double links is $4f_2$. If 6.25% of the links in a perfect lattice are replaced by double links, then 25% of the monomers will be in double links and 12.5% of the PEG arms will be used in the links (compare, with ref 10b, where ~10% of PEG is estimated to be in double links).

For effects of double links on the time course of degradation, we analyzed their impact on the formation of monomers and dimers. The gel was modeled by a modification of the diamond-lattice structure, in which it was assumed that a fraction f_2 of the adjacent pairs were double-linked. The distribution of such double-linked pairs is restricted by the necessity of removing bonds to other partners, which are then left with a potential free arm. These arms can be left dangling or can be used as additional bonds to yet other partners, transferring the bond-balance problem to those monomer subunits. The consequent restrictions on random choice of bonds to convert to double links make analytical solutions for release of oligomers $N > 2$ daunting; however, calculations for released monomers and dimers are well matched by Monte Carlo simulations (below), and thus provides some confidence that both methods are accurate for $N = 1$ and $N = 2$, and that the Monte Carlo simulations are accurate for $N > 2$.

The fraction of mass in free monomer (free dimer) at time t was estimated as follows. A monomer in the gel can initially exist in several states, depending on the initial pattern of double links, single links, and free arms associated with itself and its linked neighbors. We enumerate the initial states S relevant to calculations for the free monomer (free dimer) case, and calculate the probability $p(S)$ of each. Next, we calculate for each state the probability $p(S,t)$ at time t that the monomer is free (contained in a free dimer). Finally, the desired fraction of mass at time t is calculated as the sum for all relevant initial states of the products $p(S) \times p(S,t)$. See section S5 in the Supporting Information for details and below for comparison of analytical and Monte Carlo simulation results.

c. Degradation of Gels with Defects Caused by an Interfering Label. In earlier experiments,[2] one of the two precursors of each gel was prelabeled on a small fraction of the arms with an erosion probe, blocking those arms from forming gel bonds. In this case, the labeling itself has a direct, albeit small, effect on the rate of degradation, due to the associated increase in the proportion of initially unformed bonds. In addition, there is a more significant effect on the apparent degradation rate as compared to the actual rate. This second effect is due to an enrichment of label in released material as compared to the remaining gel. As an example, the fraction of label in monomers is q_t,[3] and the fraction of mass in monomers is q_t;[4] thus the ratio at time t is $1/q_t$ regardless of how low is the fraction of labeled arms. Analytically predicted time courses for the release of labeled polymer fragments in solution are compared to the release of mass in the presence and absence of label in Section S2 of the Supporting Information.

2. Analytical Model of Drug Release. A. Concomitant Drug Release and Gel Degradation. Because fragment—drug conjugates may be toxic, it is important to assess the amount of such conjugates present at any time. There is concomitant formation and disappearance of such conjugates, due to the drug being released from such fragments at rate k_1. To predict concomitant drug release and gel degradation, we expanded the above gel degradation model to include a drug, D, covalently attached to the gel by a linker, L1, that cleaves with rate constant k_1. As previously demonstrated,[2] we assume that the drug is released at the same rate from the intact gel and a degraded fragment. The fraction of total drug released from all species of gel components (D_{Rtot}) by time t is given by

$$D_{Rtot}(t) = 1 - e^{-k_1 t} \tag{12}$$

The fraction of total drug bound at any time t is $e^{-k_1 t}$. The fraction of total drug attached to oligomers of each size N or type is given by multiplying $e^{-k_1 t}$ with the fraction of mass for that size or type.

The free drug, D_{Rtot}, at any time t can be described using the ratios $t/t_{1/2,L2}$ and k_2/k_1, independent of absolute values of the rate constants and the time. Because $k_1 = k_2/(k_2/k_1)$ and $t = (t/t_{1/2,L2}) \ln(2)/k_2$, eq 12 can be converted to

DOI: 10.1021/acs.macromol.5b01598
Macromolecules 2015, 48, 7359−7369

$$D_{Rtot}(t) = 1 - e^{-k_1 t_F} = 1 - e^{-(\ln 2)\times(t/t_{1/2,L2})/(k_2/k_1)} \quad (13)$$

If the gel has defects, eqs 12 and 13 are still valid. Although of limited practical utility, one can calculate the amount of drug released from the intact gel vs drug fragments (Section S4 of the Supporting Information).

Next, we developed an approach to estimate the levels of soluble fragment−drug conjugates present during drug release and gel degradation. Given that the drug release rate is unaffected by fragment size,[2] the fraction of bound drug remaining is e^{-k1*t}. Thus, the fraction of total drug attached to oligomers of any size N is obtained by multiplying $e^{-k_1 t}$ by the fraction of mass for that size. The amount of drug still tethered to gel fragments at reverse gelation (D_{RG}) is $e^{-k_1 t_{RG}}$. For ideal gels, or those with no defects other than unformed bonds, eq 8 implies that amount at t_{RG} depends only on f and the ratio $r = k_1/k_2$:

$$D_{RG} = e^{-k_1 t_{RG}} = e^{-\ln(0.39/(1-f))/(k_2/k_1)} = (p_{crit})^{(k_2/k_1)} = \left(\frac{0.39}{(1-f)}\right)^r \quad (14)$$

Figure 3A shows the fraction of drug in all conjugates at t_{RG}, which is maximal unless drug release is rapid compared to gel

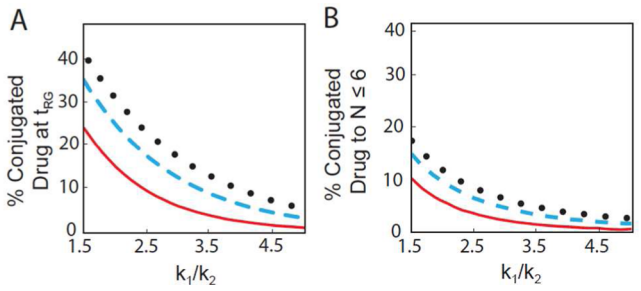

Figure 3. Fragment−drug conjugates as a function of drug release and cross-link cleavage rates. (A) Fraction of drug in free conjugates at t_{RG} for ratio k_1/k_2. The initial unformed bonds are chosen to be either f = 0 (—), f = 0.22 (---), or f = 0.30 (• • •). Each curve shows the fraction of total drug bound to conjugates at degelation ($t = t_{RG}$); see eq 14. (B) Maximum fraction of drug in small conjugates ($N \leq 6$) for ratio k_1/k_2. The initial unformed bonds are chosen to be either f = 0 (—), f = 0.22 (---), or f = 0.30 (• • •). Each point is calculated as the maximum value over time of $e^{-k_1 t}(\Sigma P_{N1-6,t})$ at the ratio k_1/k_2.

decay (e.g., $k_1/k_2 > 8$), in which case the drug on free conjugates is predominantly attached to fragments with $N \leq 6$. Figure 3B shows the maximum reached for the sum of fragment−drug conjugates of sizes up to 6; the maximum fraction of total drug attached to oligomers is estimated as the maximum of $e^{-k_1 t}P_{N\leq 6,t}$. In an ideal gel, the drug in diffusible conjugates remains below 10% when k_1 is kept above $1.5k_2$.

B. Elimination of Fragment−Drug Conjugates. In reality, physiological clearance of smaller fragment−drug conjugates from the compartment in which they form reduces the levels further. Estimation of the levels of fragment−drug conjugates considers their formation and disappearance via L1 cleavage of the drug and L2 cleavage to smaller gel fragments in a closed compartment (i.e., no net loss of total mass). For example, iIf the compartment were subcutaneous, large fragment−drug conjugates would be delivered to the circulation via the lymphatics, and subsequently eliminated by renal filtration. Glomerular filtration of PEG decreases with polymer size up to about 40 kDa, then plateaus with a $t_{1/2}$ of about 1 day in mice, 2 days in the rat, and 5 days in humans[2]. Although the clearance rate is variable and complex, it is useful to consider a simplified model to describe how to address such complexities and assign reasonable upper and lower bounds for the clearance. The simplification assumes that above a certain mass elimination can be neglected, with the large fragments trapped until further degraded. We use N_{max} to denote a number such that elimination of mass is negligible from fragments with > N_{max} monomers. Moreover, we assume that for sizes between N = 1 and N = N_{max} (eg, for 40 kDa monomers, threshold of 240 kDa and N_{max} = 6), the elimination rate can be approximated as constant with respect to mass ($P_{N\leq max}$), with rate constant k_3. Thus, the rate of change of the fraction of mass of fragments subject to elimination in the compartment of interest is equal to the rate of their production (ν_{in}) minus the rate of elimination (ν_{out}): $dP_{N\leq max}/dt = \nu_{in} - \nu_{out}$. Conjugates subject to elimination are estimated using the probability that the fragments contain unreleased drug.

In outline, the approach taken is as follows. We begin by analyzing a closed compartment where there is no elimination of fragments (i.e., $\nu_{out} = 0$), the loss of a fragment occurs only by gel bond breakage in oligomers, and all mass ultimately accumulates as monomers. First, as above in eq 1, we quantitate the monomers and small oligomer fragments released from the gel over time. Second, because the mass loss in degradation of any fragment with $N \leq N_{max}$ is balanced by production of mass in its product fragments, there is no net loss of the sum of fragments $N \leq N_{max}$ ($\nu_{out} = 0$). We therefore can calculate the net rate of production (ν_{in} for Σ(mass, $N \leq N_{max}$) for all such fragments by differentiation of the sum. Third, we now expand the model to include elimination of small fragments, $N \leq N_{max}$. We assume elimination is negligible for $N > N_{max}$, which implies that net rate of production of the sum of smaller fragments is unchanged from the rate in a closed compartment. Fourth, for convenience and of necessity, we assign a single average rate constant of elimination k_3 to the mass in the fragments with $N \leq N_{max}$; this assignment leads to a differential equation, soluble most simply by numerical methods, for the sum of mass of all sizes subject to elimination. Finally, once the remaining mass in fragments subject to elimination is quantified, drug conjugates that remain are estimated as the product of the total mass remaining and probability that it contains unreleased drug.

More specifically, for any set of oligomers of type ($N \leq N_{max}$,L,D), clearance is approximated by a first-order process with rate constant k_3. For simplicity, we assume a randomly distributed fraction f_1 of missing links, and do not consider double links; we expect the errors from this assumption to be small compared to the precision of estimates of k_3. Below, we derive equations to estimate the total fraction of mass in monomers/oligomers in sizes subject to significant elimination.

We begin with the case of a closed compartment. At time t, $P_t(N,L,D)$ is the fraction of mass in fragments of type NLD. Production of each oligomer comes from a wide range of precursors in the gel and in larger oligomers. Loss of an oligomer of a given size and type in a closed compartment comes only by bond cleavage. Ultimately, all oligimers convert to monomers and there is no loss of monomers.

From eq 1, when $k_3 = 0$, the fraction of mass in oligomers N, L, and D at time t is given by $P_t(N,L,D) = Q^* p_t^B q_t^M$, where (a) Q, B, and M are constant integers for each triple N, L, D, and (b) the parameters p_t and q_t are defined as the probability that each bond is present and absent, respectively. We assume that defects are due to a random fraction f_1 of unformed bonds,

DOI: 10.1021/acs.macromol.5b01598
Macromolecules 2015, 48, 7359−7369

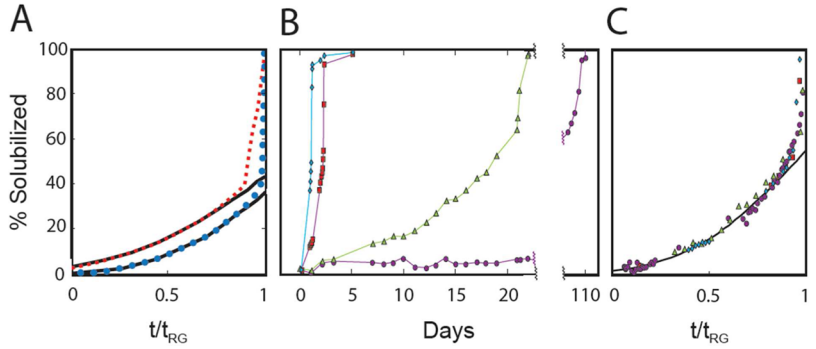

Figure 4. Comparison of time-normalized experimental degradation curves. All analytical approximations are sums using eq 5 for values of N as indicated below. (A) Comparison of time-normalized experimental degradation curves with analytical approximations; the gels are as described in entry 8 (C1) and entry 3 (C2) of Table 2 in ref 11. Curve C1 shows degradation of a homogeneous Tetra-PEG hydrogel and C2 shows degradation of a randomly formed gel in which one prepolymer was a 4-armed PEG, and the other an 8-armed PEG in which 4 arms were randomly capped prior to polymerization. Analytical approximations use $f_c(\mathrm{C1}) = 0.24$, $\Sigma P_{N_{1-6},t}$; $f_c(\mathrm{C2}) = 0.38$, $\Sigma P_{N_{1-12},t}$. (B) Reported experimental degradation curves of Tetra-PEG gels with different cleavable cross-linkers from Figure 3A of ref 2. The gels used have cleavage t_{RG} of 1.3 (♦), 2.3 (■), 22 (▲), and 105 (○) days; the data values were determined using an interfering erosion probe. (C) Normalization to t/t_{RG} of the four experimental degradation curves of the Tetra-PEG gels of B, compared to an analytical approximation (−), at $f = 0.22$, of the fractions of solubilized erosion probe (Section 1.B.c and Table SI2) in fragments of size $N \leq 12$.

implying $p_t = (1 - f_1)e^{-k_2 t}$ and $q_t = 1 - p_t$, with $\mathrm{d}/\mathrm{d}t(p_t) = -k_2 p_t$ and $\mathrm{d}/\mathrm{d}t(q_t) = k_2 p_t$. Therefore, we can derive the rate of change in $P_t(N,L,D)$, using differentiation of eq 1:

$$\frac{\mathrm{d}}{\mathrm{d}t}P_t(N, L, D) = k_2 Q p_t^{\,B} q_t^{\,M-1}(M p_t - B q_t) \tag{15}$$

Consider in contrast a compartment with elimination rate $k_3 > 0$, for fragments with $N \leq N_{max}$. Define $P_t(N \leq N_{max};k_3)$ as the probability at time t that an arbitrary monomer is contained in a fragment of size $N \leq N_{max}$; equivalently, $P_t(N \leq N_{max};k_3)$ is the fraction of mass in such fragments at time t. Further define v_{in,k_3} and v_{out,k_3} to be the rates of production and loss of $P_t(N \leq N_{max};k_3)$, respectively, resulting in eq 16:

$$\mathrm{d}/\mathrm{d}t(P_t(N \leq N_{max};\, k_3)) = (\text{rate of production, } v_{in,k_3}) - (\text{rate of loss, } v_{out,k_3}) \tag{16}$$

By assumption, the rate of loss, v_{out,k_3}, is first order with rate constant k_3:

$$v_{out,k_3} = k_3 P_t(N \leq N_{max};\, k_3) \tag{17}$$

We now calculate an expression for v_{in,k_3}, which will allow solution of eq 16 by conversion to eq 20 below. When $k_3 = 0$, there is no net loss, so $v_{out,0} = 0$. Therefore, $v_{in,0}$ can be calculated as

$$v_{in,0} = \frac{\mathrm{d}}{\mathrm{d}t}P_t(N \leq N_{max};\, 0) = \sum_{N \leq N_{max}} \sum_{L,D} \frac{\mathrm{d}}{\mathrm{d}t}P_t(NLD) \tag{18}$$

When $k_3 > 0$, we assume negligible loss for sizes $N > N_{max}$ implying $v_{in,k_3} = v_{in,0}$; in other words, the net rate of production of the sum of oligomers of smaller sizes ($N \leq N_{max}$) from larger oligomers ($N > N_{max}$) is the same as for the closed compartment. Combining this equality with eqs 15 and 18 gives v_{in,k_3} as a polynomial in p_t and q_t (where Q, B, and M in each term depend as usual on the triple NLD):

$$v_{in,0} = \frac{\mathrm{d}}{\mathrm{d}t}P_t(N \leq N_{max};\, 0) = \sum_{N \leq N_{max}} \sum_{L,D} \frac{\mathrm{d}}{\mathrm{d}t}P_t(NLD) \tag{19}$$

The small-fragment mass, $y = P_t(N \leq N_{max};k_3)$, is therefore determined by a simple first-order differential eq 18. The right side is a polynomial in p_t and q_t (since M is always >1, the exponent $M - 1$ is positive), and so is also a polynomial in the exponential $e^{-k_2 t}$:

$$y' + k_3 y = k_2 \times \sum_{N=1}^{N\max} \sum_{LD} Q p_t^{\,B} q_t^{\,M-1}(M p_t - B q_t)] \tag{20}$$

Because $q_t = 1 - p_t$, we can view this relationship more simply as

$$y' + k_3 y = k_2 F(p_t) \tag{21}$$

where $F(p_t)$ is a polynomial in p_t.

The choice of N_{max} is based on the compartment of interest. For each such case, eq 21 implies that the time course of elimination of mass (when scaled as a function of $t/t_{1/2}$ or t/t_{RG}) depends only on the quality of the gel and the choice of the ratio k_3/k_2; see Section 6, Supporting Information, for more details.

The total mass remaining in the compartment, including both gel and fragments of all sizes, can now be calculated. The only loss is from small fragments $N \leq N_{max}$, so the fraction of total mass remaining is given by the sum of $[1 - P_t(N \leq N_{max};0)]$ (all mass not degraded to fragments $N \leq N_{max}$) and $P_t(N \leq N_{max};k_3)$ (the uneliminated remnant of fragments $N \leq N_{max}$).

$$\mathrm{mass}_{t,k_3} = [1 - P_t(N \leq N_{max};\, k_3)] + P_t(N \leq N_{max};\, k_3) \tag{22}$$

The total conjugated drug remaining at time t and the conjugated drug on small fragments ($N \leq N_{max}$) are given respectively by multiplying $e^{-k_i t}$ with total remaining mass (mass_{t,k_3}) and small fragment mass ($P_t(N \leq N_{max};k_3)$).

The level of free drug in the compartment is also affected by the elimination of conjugates as well as by its own elimination. For the free drug D_t, we approximate its direct elimination as a first-order process, with rate constant $k_{3,drug}$. Under this assumption, D_t satisfies the first order differential equation that incorporates the effect of conjugate elimination:

DOI: 10.1021/acs.macromol.5b01598
Macromolecules 2015, 48, 7359−7369

$$\frac{\mathrm{d}}{\mathrm{d}t}D_t = k_1 \times \text{conj-drug}_{t,k_3} - k_{3,drug} \times D_t \quad (23)$$

Equation 23 can be solved using the values for total conjugated drug (conj-drug$_{t,k3}$ = e$^{-k_1 t}$mass$_{t,k_3}$) based on eq 22.

3. Analytical Approximation of Experimental Degradation Curves. We assessed the degree to which degradation can be approximated by analytical curves considering only missing bonds. By applying eqs 1−5, each fraction f quantifying the missing bonds determines analytical curves for degelation, $C_{f,N_{max}}(t) = \Sigma P_{N\leq Nmax,t}$. As described above, before the onset of reverse gelation of high-quality gels, the formation of fragments with $N > 6$ is insignificant, and there is near-quantitative release of fragments of size $N \leq 6$ from the gel. For each experimental curve C, we determine an optimal value of f, f_C, by minimizing the standard deviation of the residuals between the experimental curve and the analytical curve $\Sigma P_{N_{1-6},t}$ up to the point at which $C_{f,6}$ diverges from $C_{f,12}$.

Figure 4A shows two experimental degradation curves for hydrogels[11], one Tetra-PEG and one in which one prepolymer is 4-arm PEG, while the other is an 8-arm PEG in which an average of 4 arms per subunit were randomly capped prior to polymerization. For curve C1, $f_C = 0.24$ (±0.1); the close match of the optimal calculated curve to the data extends to $0.85t/t_{RG}$ (SD of residuals <0.004) suggesting that most larger fragments formed are trapped until near t_{RG}. For curve C2, $f_C = 0.38$ (±0.2). The data matches $\Sigma P_{N_{1-6},t}$ until the curve $\Sigma P_{N_{1-12},t}$ diverges from $\Sigma P_{N_{1-6},t}$ and continues to closely match the curve $\Sigma P_{N_{1-12},t}$ up to $0.90t/t_{RG}$ (SD of residuals 0.009). The random capping of half of the arms of the 8-armed PEG produces a mix of prepolymers with 0−8 reactive end groups. The resulting gel should have many units linked to fewer than 4 other units. In the degradation curve, the loss of mass in relation to t/t_{RG} has 2.24-fold increased area under the curve up to 0.7.[11]

The number f_C for an experimental gel is determined only by the degradation curve; it is a measure of gel quality, affected by imperfections that influence degradation rate. A similar but nonidentical measure proposed by the Sakai group[10a] is the reaction efficiency p, measured as the fraction of active termini forming bonds; for example, p for 5% Tetra-PEG gels was measured to be in the range 0.78−0.9,[12,10a] consistent with $f \sim 1 - p$.

Figure 4B shows four reported degradation curves for homogeneous Tetra-PEG gels with t_{RG} of ∼1 to 100 days, as determined using an interfering erosion probe (Figure 3A in[2]). The curves, when replotted in Figure 4C as fraction total label vs t/t_{RG}, are essentially identical, indicating that the gels are of similar quality despite having disparate t_{RG}'s. Simulations of the fraction of label in fragments of size $N \leq 12$ were determined using the approach described in Sections 1.B.c and S2 of the Supporting Information. The best match for the combined data sets provided $f_C = 0.22$ as the estimate of gel quality, matching the experimental data closely to about 85% of t_{RG}. After further correcting for an estimated 2% increase in the unformed bonds due to the labeling, the estimate of quality becomes ∼0.20. Using $f = f_C$ in eqs 1−5 allows prediction of the degradation curve for fraction of mass in the solubilized oligomers; as previously described (section I.1.B.c), measurement of degradation via an erosion probe overestimates mass released.

II. Monte Carlo Simulations. To test and potentially expand the analytical theory, we also developed a Monte Carlo model of gel degradation and drug release. When both are applicable, the two approaches deliver essentially identical results, thus increasing our confidence in each. In addition, the Monte Carlo approach is used to analyze a more complex range of gel imperfections.

1. Simulations of Hydrogel Degradation. A. Fragment Formation during Degradation. In addition to analytical calculations, Tetra-PEG degradation was simulated by a Monte Carlo method that iteratively introduced a large number of random L2 cross-link cleavages, as follows. The gel was represented by a graph of connected nodes using the NetworkX v1.7 software package.[13] Each monomer corresponded to a node in the graph, and each L2 cross-link to an edge between two nodes. As in the analytical approach, the probability of an L2 cross-link of the polymer to be cleaved at each time step (t) is $P = 1 - e^{-k_2 t}$; the simulations were performed using k_2 values ranging from 0.005 to 1.0 day^{-1}. L2 cleavage was modeled by removal of the cleaved edge in the graph, eventually splitting the graph into subgraphs. Each subgraph corresponded to an oligomer with a variable number of monomers formed within the gel. Finally, for each $N \leq 6$, the number of oligomers with N monomers was counted, multiplied by N, and then divided by the initial total number of monomers to give the fraction of the total mass in oligomers of size N; these fractions were summed to give the fraction of the total $N \leq 6$ oligomer mass.

Because the simulated system is by necessity of finite size, we improved the accuracy and precision of our simulations in two ways. First, for each set of conditions, the behavior of the system was determined by averaging 50 independent simulation runs. Second, to minimize the finite size boundary effects, the polymer resided in a cubic unit cell surrounded face on face with 6 identical symmetry unit cells, thus creating a cubic symmetry lattice with a periodic boundary condition; each surface monomer with less than four links was linked to its nearest neighbor(s) in a neighboring symmetry unit cell. The results shown are those for simulations of polymers consisting of 500 4-arm PEG monomers of each type. Simulations of polymers ranging from 250 to 8000 monomers in the unit cell demonstrated similar degradation properties (data not shown).

The results from the analytical method were presented as a function of the fraction of time $t/t_{1/2,L2}$, while Monte Carlo simulations were performed for specific values of k_2 and the fractions of $N \leq 6$ oligomers plotted as a function of time t. To compare the two methods, we therefore converted the Monte Carlo simulation time into fractions of time $t/t_{1/2/,L2}$. The degradation curves from the analytical theory and the Monte Carlo simulations fit each other perfectly for a number of different conditions (Figure 5A; data not shown).

B. Effect of Gel Defects on Degradation. As described for the analytical approach, the MC model was used to describe gel defects in Tetra-PEG gels arising from unformed bonds and primary double links.

a. Unformed Bonds. To simulate gel imperfections arising solely from an absence of some of the cross-links, we randomly removed a fixed percentage of cross-links from an ideal polymer at the outset and repeated the simulations. Again, the Monte Carlo and analytical models provided identical profiles.

b. Primary Double Links. In the analytical approach, gel degradation in the presence of double links could only be modeled for $N \leq 2$. In contrast, the Monte Carlo approach does not suffer from this limitation. Three different algorithms were used to build polymers with varying fractions of double links and unformed cross-links (Section 6a of the Supporting

DOI: 10.1021/acs.macromol.5b01598
Macromolecules 2015, 48, 7359−7369

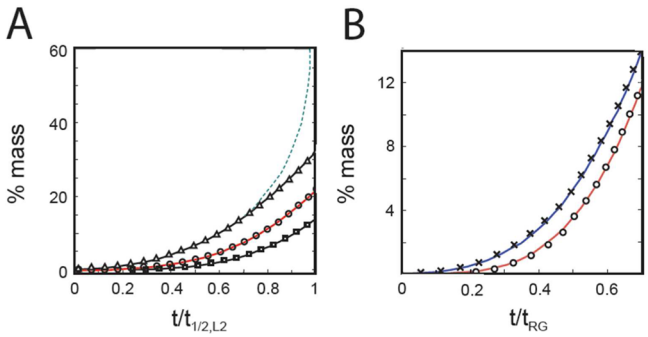

Figure 5. Comparison of the analytical and Monte Carlo approaches. All Monte Carlo degradation curves were obtained with a kinetic rate constant of 0.006 $days^{-1}$ and a time step of 1 day. (A) Gel degradation as measured by mass loss, computed using analytical theory (eq 5 and Table S2 of the Supporting Information) (continuous lines) and Monte Carlo simulations (Δ, ○, □) of an ideal gel (□), a gel with 10% incomplete cross-links (○), and by an erosion probe attached to 10% of the end groups (Δ). Simulated lines fit experimental results (below) up to near t_F. Also shown (gray dotted line) is a hand-drawn depiction of the expected acceleration between t_F and t_{RG}. (B) Simulated gel degradation as measured by mass loss ($N \leq 6$ oligomers) of gels with 40% of monomers in double bonds and either no broken bonds (○) or 10% broken bonds (**x**) compared to analytical degradation curves (solid lines) for gels with no double bonds and either 3% broken bonds (through ○) or 14% broken bonds (through **x**).

Information). The first algorithm was devised to change an ideal lattice minimally. To construct a polymer with a given fraction of double links, a set of nonintersecting paths in the ideal network was chosen; in each path, alternating links are doubled and the intervening links deleted. The second algorithm was devised to change an ideal lattice maximally, while avoiding long-range links. The third algorithm was intermediate between the first two; it sequentially modifies an ideal lattice, with each step limited to making changes between nodes within a fixed network distance.

Monte Carlo modeling of degradation for mass loss of $N \leq 2$ perfectly matched that calculated using the analytical approach (data not shown). In addition, the Monte Carlo approach was used to simulate degradation to $N \leq 6$. For example, we simulated mass loss for $N \leq 6$, starting from a polymer with 40% of monomers in double links, but no free arms (Figure 5B). The resulting degradation curve was compared to the analytical curves for an ideal gel modified by varying fractions f of unformed bonds. The simulated degradation curve closely approximates the analytical degradation profile of a near-ideal Tetra-PEG gel (3% broken bonds; SD of residuals ~0.0012 over the range $0-0.7t_{RG}$), suggesting that double links in an otherwise ideal gel only slightly affect degradation. We also simulated the degradation of polymers with 10% broken bonds and varying amounts of double links. The combination of double links between 40% of monomers and 10% unformed links increases the degradation only slightly compared to that for 10% broken bonds alone, with the best match to polymer with no double links having 14% broken bonds (SD of residuals ~0.0006 over the range $0-0.7t_{RG}$). Hence, the degradation curves in the presence of double links appear to be well modeled by analytical curves derived from the assumption of broken bonds alone.

c. Degradation of Gels with Defects Caused by an Interfering Label. As in the analytical approach (Figure 5A), we computed the loss of an erosion probe randomly and irreversibly attached to a small fraction of the arms of one of the Tetra-PEG units using Monte Carlo simulations. The label amount attached to fragments of size $N \leq 6$ was counted at each time step, and the fraction of total labels was plotted as a function of fraction of time $t/t_{1/2,L2}$. As for other comparisons above, the analytical and Monte Carlo methods provided identical results (Figure 5A).

2. Monte Carlo Simulations of Drug Release. A. Concomitant Drug Release and Gel Degradation. We also employed Monte Carlo simulations to analyze concomitant drug release and gel degradation. A drug was attached to the gel, modeled as described above, via L1 linkers having cleavage rate constant k_1. The unit cell of the resulting drug-polymer model had 1000 nodes. Simulations were performed using a fixed k_2 value of 3×10^{-5} day^{-1} and varying k_1 to produce k_2/k_1 ratios ranging from 0.05 to 0.35 in 0.05 increments. At each time t, we counted the total fraction of free drug, the carrier origin of the free drug, and the fraction of the drug bound to oligomers of size $N \leq 6$. In all cases, the Monte Carlo simulation of the time course of each of the measured quantities matched the analytical curves (data not shown).

■ DISCUSSION

We previously reported a drug-delivery system that uses sets of self-cleaving β-eliminative linkers to tether drugs to and cross-link Tetra-PEG hydrogels. By using one β-eliminative linker to attach the drug and another with a longer half-life of cleavage to control polymer degradation, the drug delivery system can be designed to release the drug before the gel undergoes significant degradation. The design requires balancing the rates of drug release and gel degradation, k_1 and k_2, respectively, so that insofar as possible, three objectives are attained: (a) the drug is mostly released before significant gel degradation occurs, (b) released fragment−drug conjugates are minimized, and (c) the period until the gel dissipates is short so it does not remain at the injection site for prolonged periods. In the present work, we describe analytical calculations and Monte Carlo simulations of the concomitant release of drugs from and degradation of Tetra-PEG hydrogels. The concordance of the two approaches and comparison to experiment attest to their validities.

Summary of Simulations. First, we simulated the formation of gel fragments of various sizes through the course of gel degradation. We show that most of the fragments formed early in an ideal diamond lattice consist of oligomer sizes $N \leq 6$; only a small increase occurs if larger oligomers $N \leq 12$ are considered. Assuming that fragments of $N \leq 6$ freely diffuse through the gel, we estimated total mass loss up to 70% of $t_{1/2}$ of the cross-linker L2 as the sum of such fragments. Significant amounts of larger oligomers are created after this period, which may or may not escape the gel before complete solubilization.

We performed similar simulations after introduction of unformed bonds and/or primary double links into the lattice. Unformed bonds arise from topological restrictions or destruction of reactive components of connecting end-groups, especially if susceptible to hydrolysis. Formation of double links is expected to be governed by concentration of polymer components, and enhanced by dilute solutions during polymerization[10b]. We estimated the effects of such defects on the fraction of intact bonds needed to maintain the gel and on the relationship between $t_{1/2,L2}$ and t_{RG}. In general, our simulations indicate that unformed bonds increase the apparent rate of degradation to shift the degradation curve to the left (Figure

DOI: 10.1021/acs.macromol.5b01598
Macromolecules 2015, 48, 7359−7369

2B), and significantly reduce t_{RG}. For gels containing double links, we performed analyses of monomer and dimer formation. Since these represent the greatest fraction of released mass over early times, they are a reasonable estimate of the behavior of degradation. The difficulty in describing the distribution of double bonds in higher oligomers makes analytical solutions daunting. However, the MC model reproduced the analytical results for monomers and dimers, and enabled the analysis of gels containing double links to at least $N \leq 6$. Overall, double links reduced the t_{RG} of near-ideal gels only slightly and had only a small effect on the degradation curve (mass lost vs t/t_{RG}), which could be approximated in the range studied by assumption of a small increase in the fraction of unformed bonds. The minimal effect of double links on apparent degradation rates is due to compensatory effects: an oligomer of a specific size in the presence of double links is easier to create because, on average, fewer bonds need to be broken; however, it is harder to break down, because, on average, additional bonds need to be broken.

Second, we simulated the drug released from the intact gel and gel fragments in context of a continuously degrading gel. We described loss of drug from the intact gel and $N \leq 6$ fragments over the degelation period using the ratios $t/t_{1/2,L2}$ and k_2/k_1, independent of absolute values of the rate constants and time.

Third, we estimated the amount of fragment−drug conjugates present as a function of drug release and gel degradation rates. For hydrogel containing up to ∼20% unformed or double bonds we calculated an upper limit of the amount of drug attached to all fragments as a function of k_1/k_2. We calculated an upper bound for the amount of drug attached to released fragments with $N \leq 6$ as a function of k_1/k_2. For example, Figure 3A,B shows that at $k_1/k_2 = 1.5$ no more than 10% of drug is attached to soluble fragments at any time, the maximum occurring at t_{RG}. The levels can be reduced by simply increasing k_1/k_2. We also showed that for a given k_1/k_2, the maximum amount of fragment−drug conjugate present at any time decreases as the network structure approaches a more ideal lattice structure.

Finally, we describe an approach to estimate the fragment−drug conjugates in a compartment where fragments below a specified size can be cleared. After calculating the time course of clearable fragment mass in the absence of elimination, we calculate the rate of production of such fragments. We then incorporate an estimate of the clearance rate for clearable mass to calculate the mass lost from the compartment, as well as the time course of clearable mass remaining. Assuming rates of fragment production and loss to be independent of the presence of conjugated drug, the conjugates in each compartment are then calculated.

Practical Utility of the Models. A main purpose of this work was to characterize the dynamics of in vivo drug release and gel degradation in the Tetra-PEG DDS we have developed.[2,14] The relevant considerations depend on whether the compartment in which the gel is administered is the site of action and/or potential toxicity, or whether those occur in a compartment to which components are delivered. If the injection compartment serves as a depot, the major consideration is what leaves that compartment and enters the other. For example, in a subcutaneous (s.c.) injection, the major concern regarding efficacy or toxicity is generally not what remains at the site of injection, but rather what enters the systemic circulation (e.g., drug, PEG fragments, fragment−drug conjugates). On the other hand, if the compartment is the site of action and/or potential toxicity, components retained in the compartment are the major issue. For example, in an intravitreal injection, the major concern would be the components retained in the eye and their local effects. The large dilution that occurs when components leave the eye (∼4 mL) and enter the circulation would likely nullify potential systemic effects of these components.

A simplified, general PK model of the DDS is shown in Figure 6. As before, k_1 and k_2 are rate constants for drug release

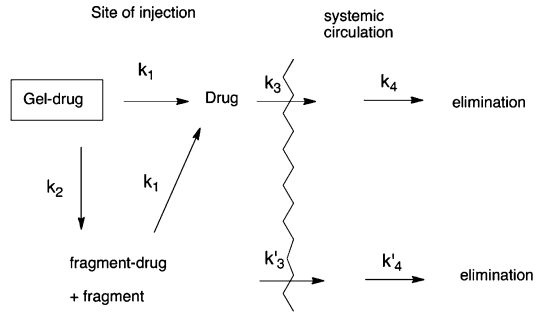

Figure 6. Pharmacokinetic model of a degrading Tetra-PEG DDS in a semipermeable compartment.

and cross-linker cleavage, respectively. k'_3 and k_3 are the rate constants for transfer of drug and gel fragments of defined sizes (e.g., $N \leq 6$), respectively, from the local compartment into the central compartment, where drug and gel fragments are ultimately eliminated, with rate constants k_4 and k'_4, respectively, by renal filtration or other process. The controllable variables include k_1 and k_2, and thus k_1/k_2, and in some cases k'_3 by control of the size of the monomer components of the gel.

An effective way to illustrate the dynamics of the system is to consider concentration vs time (C vs t) profiles of the products of a degrading Tetra-PEG DDS in a compartment of interest. For this purpose, we use a example with $k_1/k_2 = 3$, and consider the behavior in a closed system. Then, rates of elimination pathways of drug, gel, and gel−drug fragments are estimated and modifications of the dynamics are compared to that of the closed compartment.

First, we consider the dynamics of the DDS in a closed system; here, there is no pathway for elimination of degradation products, and the gel-drug is ultimately converted to free drug and the two PEG monomers. Although completely closed systems are rare in vivo, the system serves as a basis for comparisons with natural compartments and describes degradation behavior in common laboratory experiments. Figure 7A shows C vs t curves of various degradation products of the model DDS where k_1/k_2 was arbitrarily chosen as 3. The free drug accumulates in a first-order process dependent only on k_1. In the early period, the total mass of large fragments of $N > 6$ is very low, and then slowly increases. Shortly before t_{RG} the remaining gel erodes with increasing speed into increasingly larger fragments of $N > 6$ until solubilization. Then, the mass in large fragments decreases as they convert to smaller fragments of $N \leq 6$ and ultimately to accumulated monomers. The drug in fragment−drug conjugates is the product of fragment mass and the exponentially decreasing fraction of bound drug. In the specified case where the rate of drug release, k_1, is 3-fold higher than the rate of cross-linker cleavage, k_2, there is low accumulation of drug-fragment conjugates. Large fragments N

DOI: 10.1021/acs.macromol.5b01598
Macromolecules 2015, 48, 7359−7369

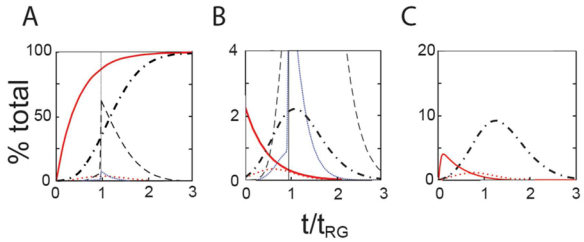

Figure 7. Analytical models of drug, conjugates and degraded fragments in various compartments in the absence and presence of elimination. (A) Closed compartment showing fraction of initial mass or drug vs t/t_{RG} in free drug (red −), fragments of size $N \leq 6$ (— • —) or $N > 6$ (- - -), and free conjugates $N \leq 6$ (red dots) or $N > 6$ (blue dots). (B) Small semipermeable local compartment with permeability insignificant for $N > 6$ showing same forms as panel A. (C) Central compartment after delivery of drug from a semipermeable subcutaneous compartment with permeability insignificant for $N > 6$; the same forms are shown, for free drug, fragments of size $N \leq 6$ and fragment-conjugates $N \leq 6$. Note that the central compartment in panel C is much larger than the local compartment of B; thus, although the fraction of a component in the small local compartment is low, the concentration will be significantly higher. $f = 0$ (—), $f = 0.22$ (---), or $f = 0.30$ (• • •).

> 6 contain only a small amount of drug because most of the drug is released before large fragments are created; such conjugates reaches a maximum at t_{RG} − in the example ∼10%. The fraction of drug bound to small fragments $N \leq 6$ also remains low; in the example case, the fraction of drug bound to small fragments reaches a maximum of only 6% shortly after t_{RG}.

Next, we consider the dynamics of the DDS when injected into a semipermeable localized compartment; examples of such would be the eye or intra-articular spaces. This case is similar to the closed compartment, except there is elimination of free drug, k_3, and small gel and gel-drug fragments, k'_3. Since there is a large dilution of components on entry to the systemic circulation, the major concern regarding efficacy or toxicity of components is usually in the initial compartment of injection. Figure 7B shows hypothetical C vs t plots of degradation products in a small, localized compartment (e.g., 4 mL for eye or synovial fluid of knee). Here, we arbitrarily assume that $t_{1/2}$ of drug release (k_1) is 20 days, $t_{1/2}$ of gel bonds (k_2) is 60 days (i.e., $k_1/k_2 = 3$) and is approximately the same as the t_{RG}, that drug (k_3), smaller fragments of $N \leq 6$ (k'_3) all leave the compartment with $t_{1/2}$= 1 day. As shown, the free drug level is governed by the balance between rate of its release from the gel or fragment−drug conjugates (k_1), and rate of elimination of drug into the systemic compartment (k_3). The mass of large fragments resembles that in a closed compartment; it reaches a maximum at t_{RG}, then decreases as it dissipates into smaller fragments. Nearly 90% of the burden of gel mass remaining from a single dose is eliminated within 2 t_{RG} and complete removal occurs by $3t_{RG}$. The masses of small permeable fragments of $N \leq 6$, are determined by the balance between rate of production by gel decay (k_2) and rate of elimination from the compartment (k'_3). With loss from the compartment, small gel−drug fragments, already low in the closed compartment, never account for more than 1% of the total drug administered. To obtain steady-state levels after multiple injections one simply performs superposition of the single-dose curves.

Finally, we consider the dynamics of the DDS when injected subcutaneously for systemic administration of the drug. In contrast to the above, the major concern is not what remains at the site of s.c. injection, but rather what enters the systemic compartment containing the sites of action and potential toxicity. Once released from the gel, the free drug will enter the circulation either by penetrating blood vessels or via the lymphatic system (k_3). Figure 7C shows ta hypothetical C vs t plot of drug, gel oligomers and fragment−drug complexes in the blood compartment. In the simulation, we employed the same values for k_1, k_2, k_3, and k'_3 as in Figure 6B; in addition, we used $t_{1/2}$ values of 1 day and 5 days for elimination of drug (k_4) and PEG fragments (k'_4) from the central compartment. The free drug in circulation increases as a function of k_1 and k_3 and then decreases as a function of k_4. Large fragments are absent because they do not leave the injection site. Smaller PEG fragments enter from the injection compartment (k'_3) and leave by renal elimination (k'_4). The fragment−drug complexes are low, remaining below 1.5% of the total drug administered. As before, steady-state levels of components after multiple injections can be obtained by superposition of the single-dose curves.

In conclusion, we have provided complementary approaches for analytical calculations and Monte Carlo simulations of the degradation of Tetra-PEG hydrogels tethered to a releasable drug. The models produce accurate estimates of free drug, gel fragments and gel fragment−drug complexes through the course of gel degradation. We have illustrated how the approaches can be used to model components of the DDS in various compartments.

Most information obtained by simulations would be difficult or impossible to determine experimentally. In addition to designing gels with desirable properties, the simulations allow avoidance of potential complications that may hinder FDA approval. For example, if the FDA considers small drug-fragment conjugates as metabolite impurities, then no more than 10% may be present in this form without thorough characterization−a daunting task in view of the heterogeneous nature of such conjugates.

We estimate that in a single Tetra-PEG hydrogel microsphere there are about 10^{11} covalently linked monomers, and gels of current interest contain up to two drug molecules/PEG monomer.[2] At the point of reverse gelation approximately 50% of the cross-linked bonds are cleaved, leaving very large polymeric structures. Functionally, the drug on large polymer-drug conjugates behaves as does the gel-drug conjugate: that is, the drug will largely remain localized until smaller drug-fragments are formed, and be devoid of biological activity.

■ ASSOCIATED CONTENT

Supporting Information

The Supporting Information is available free of charge on the ACS Publications website at DOI: 10.1021/acs.macromol.5b01598.

Materials and methods and detailed descriptions of the analytical and Monte Carlo models (PDF)

■ AUTHOR INFORMATION

Corresponding Author

*(D.V.S.) E-mail: daniel.v.santi@prolynxllc.com.

DOI: 10.1021/acs.macromol.5b01598
Macromolecules 2015, 48, 7359−7369

Notes

The authors declare the following competing financial interest(s): Two authors are employees and shareholders of ProLynx LLC (D.V.S., R.R.).

■ ACKNOWLEDGMENTS

This work was supported by NSF SBIR Grant No. 1429972, M.S. was supported by a SPINNER 2013 (Global Grant of the Emilia-Romagna Regional Operative Programme (ROP) 2007-2013, European Social Fund (ESF), Axis IV Human Capital Objective 2 "Regional Competitiveness and Employment") fellowship.

■ REFERENCES

(1) (a) Sakai, T. Experimental verification of homogeneity in polymer gels. *Polym. J.* **2014**, *46*, 517−523. (b) Sakai, T. Gelation mechanism and mechanical properties of Tetra-PEG gel. *React. Funct. Polym.* **2013**, *73*, 898−903. (c) Sakai, T.; Matsunaga, T.; Yamamoto, Y.; Ito, C.; Yoshida, R.; Suzuki, S.; Sasaki, N.; Shibayama, M.; Chung, U.-i. Design and Fabrication of a High-Strength Hydrogel with Ideally Homogeneous Network Structure from Tetrahedron-like Macromonomers. *Macromolecules* **2008**, *41*, 5379−5384.

(2) Ashley, G. W.; Henise, J.; Reid, R.; Santi, D. V. Hydrogel drug delivery system with predictable and tunable drug release and degradation rates. *Proc. Natl. Acad. Sci. U. S. A.* **2013**, *110* (6), 2318−23.

(3) Flory, P. J. *Principles of polymer chemistry*. Cornell University Press: Ithaca, NY, 1953; p 672.

(4) Li, X.; Tsutsui, Y.; Matsunaga, T.; Shibayama, M.; Chung, U.; Sakai, T. Precise Control and Prediction of Hydrogel Degradation Behavior. *Macromolecules* **2011**, *44*, 3567−3571.

(5) Rydholm, A. E.; Reddy, S. K.; Anseth, K. S.; Bowman, C. N. Development and Characterization of Degradable Thiol-Allyl Ether Photopolymers. *Polymer* **2007**, *48* (15), 4589−4600.

(6) DuBose, J. W.; Cutshall, C.; Metters, A. T. Controlled release of tethered molecules via engineered hydrogel degradation: model development and validation. *J. Biomed. Mater. Res., Part A* **2005**, *74* (1), 104−116.

(7) Lao, L. L.; Peppas, N. A.; Boey, F. Y.; Venkatraman, S. S. Modeling of drug release from bulk-degrading polymers. *Int. J. Pharm.* **2011**, *418* (1), 28−41.

(8) (a) Stauffer, D.; Aharony, A. *Introduction to Percolation Theory*. Taylor & Francis: Philadelphia, 1992. (b) Essam, J. W. Percolation and Cluster Size. In *Phase Transitions and Critical Phenomena*; Academic Press: New York, 1972; Vol. *2*, pp 197−270.

(9) (a) Grimmett, G. *Percolation*. 2nd ed.; Springer-Verlag: Berlin, 1999;. (b) Bollobás, B.; Riordan, O. *Percolation*. Cambridge University Press: Cambridge, U.K., 2006.

(10) (a) Akagi, Y.; Katashima, T.; Katsumoto, Y.; Fujii, K.; Matsunaga, T.; Chung, U.-i.; Shibayama, M.; Sakai, T. Examination of the Theories of Rubber Elasticity Using an Ideal Polymer Network. *Macromolecules* **2011**, *44*, 5817−5821. (b) Lange, F.; Schwenke, K.; Kurakazu, M.; Akagi, Y.; Chung, U.-i.; Lang, M.; Sommer, J.-U.; Sakai, T.; Saalwachter, K. Connectivity and Structural Defects in Model Hydrogels: A Combined Proton NMR and Monte Carlo Simulation Study. *Macromolecules* **2011**, *44*, 9666−9674.

(11) Henise, J.; Hearn, B. R.; Ashley, G. W.; Santi, D. V. Biodegradable Tetra-PEG Hydrogels as Carriers for a Releasable Drug Delivery System. *Bioconjugate Chem.* **2015**, *26*, 270.

(12) Akagi, Y.; Matsunaga, T.; Shibayama, M.; Chung, U.; Sakai, T. Evaluation of Topological Defects in Tetra-PEG Gels. *Macromolecules* **2010**, *43*, 488−493.

(13) Hagberg, A. A.; Schult, D. A.; Swart, P. J. In *Exploring network structure, dynamics, and function using NetworkX*, Proceedings of the 7th Python in Science Conference (SciPy2008), Pasadena, CA, Varoquaux, T., Vaught, T., Millman, J., Ed.; SciPy: Pasadena, CA, 2008; pp 11−15.

(14) Santi, D. V.; Schneider, E. L.; Reid, R.; Robinson, L.; Ashley, G. W. Predictable and tunable half-life extension of therapeutic agents by controlled chemical release from macromolecular conjugates. *Proc. Natl. Acad. Sci. U. S. A.* **2012**, *109* (16), 6211−6.

DOI: 10.1021/acs.macromol.5b01598
Macromolecules 2015, 48, 7359−7369